Quantum Electronics **47** (3) 222–227 (2017)

https://doi.org/10.1070/QEL16317

Quasi-classical model of electron rescattering in fields of intense infrared and weak high-frequency laser pulses

A.V. Flegel, M.V. Frolov, A.N. Zheltukhin, N.V. Vvedenskii

Abstract. **We study the influence of a weak high-frequency [in the extreme ultraviolet (XUV) region] laser pulse on the mechanism of electron rescattering on the parent ion in the processes of high harmonic generation and above-threshold ionisation induced by an intense infrared (IR) laser field. Two scenarios of the three-step rescattering are discussed: with the absorption of the XUV photon at the ionisation step of an atom and with the absorption/emission of a XUV photon at the moment of recombination or scattering of the electron returned by the IR field to the parent ion. Estimates are obtained for the high-energy plateau cutoff positions in the spectra of harmonic generation and above-threshold ionisation.**

Keywords: *high-harmonic generation, above-threshold ionisation, quasi-classical rescattering model, strong laser field, analytical theories.*

1. Introduction

When an intense laser field interacts with atomic systems, one can observe plateau-like structures in the spectrum of high harmonic generation (HHG) and in the spectrum of above-threshold ionisation (ATI) of atoms: in the case of HHG, plateau-like structures exhibit a weak dependence of the harmonic generation efficiency on the harmonic frequency, and in the case of ATI – a weak dependence of the yield of high-energy electrons on their energy. The physics of plateau effects in strong low-frequency fields is determined by the quasi-classical three-step rescattering model [1–4]: in the course of tunnelling, an atomic electron undergoes a transition from the bound state to the state of a continuum with zero energy; then, a strong oscillating laser field 'picks up' the released electron and returns it to the original atomic core along a closed trajectory, where the electron either gains an additional energy from the laser field during the rescattering process, thereby forming a high-energy plateau in the ATI spectra, or recombines with the parent ion with the emission of a hard photon (harmonic), thereby releasing the energy gained during the motion along this closed trajectory.

A.V. Flegel Voronezh State University, Universitetskaya pl. 1, 394018 Voronezh, Russia;
M.V. Frolov Voronezh State University, Universitetskaya pl. 1, 394018 Voronezh, Russia; Institute of Applied Physics, Russian Academy of Sciences, ul. Ul'yanova 46, 603950 Nizhnii Novgorod, Russia;
A.N. Zheltukhin, N.V. Vvedenskii Institute of Applied Physics, Russian Academy of Sciences, ul. Ul'yanova 46, 603950 Nizhnii Novgorod, Russia; e-mail: vved@appl.sci-nnov.ru

Received 9 February 2017
Kvantovaya Elektronika **47** (3) 222–227 (2017)
Translated by I.A. Ulitkin

The addition of a weak extreme ultraviolet (XUV) field to an intense infrared (IR) field can substantially modify the spectra of the induced processes. For example, the authors of papers [5, 6] demonstrated the possibility of a substantial broadening of the HHG spectra due to a shift of the plateau cutoff to the region of high-order harmonics, as well as due to an enhancement of individual harmonic groups [5, 7]. Recently, studies of ultrafast processes using XUV-initiated high harmonic generation (XIHHG) have been of particular interest [8, 9]. Unlike HHG in a strong low-frequency field, XIHHG is initiated by the absorption of a hard photon by an electron on the inner shell of the atom, followed by the formation of a vacancy and emission of an electron into the continuum. During the movement along a closed trajectory, the formed vacancy of the atomic core 'migrates' in it. A temporary vacancy migration can be recorded by measuring the yield of harmonics at different frequencies [10, 11]. In the case of ATI, the combination of IR and XUV pulses was mainly used in attosecond metrology [12, 13].

Quantum-mechanical amplitudes of HHG and ATI can be analysed by using a quasi-classical (adiabatic) approach. In the framework of this approach, of importance is the calculation of the times of ionisation and return (rescattering) of the electron to the parent ion and, accordingly, the time of motion of the electron along the closed classical trajectory between the ionisation and rescattering moments [14, 15]. In the presence of an additional XUV pulse, a quasi-classical analysis of the amplitudes of the processes shows that additional channels of ionisation and (or) excitation of an atomic target induced by a high-frequency pulse cannot be taken into account in the framework of the commonly accepted adiabatic approach. The most consistent account for these channels is possible within the framework of perturbation theory with respect to the intensity of a high-frequency pulse against the background of a nonperturbative interaction of a low-frequency field with an atomic target.

In this paper we analyse a quasi-classical model of rescattering with allowance for a weak XUV pulse in the first order of perturbation theory. For this case, the following rescattering scenarios are possible, taking into account ionisation, excitation or de-excitation of an atomic target:

1. An atomic electron absorbs a XUV photon and passes into a continuous spectrum in which an electron is 'picked up' by a strong laser field and moves along a closed classical trajectory. At the last step, the electron recombines (in the case of HHG) or is scattered on the atomic core (in the case of ATI).

2. An atomic electron tunnels in a strong low-frequency field and moves along a closed trajectory. At the last step, it recombines or is scattered in the field of a high-frequency

pulse, followed by emission or absorption of a XUV photon at the carrier frequency of a high-frequency pulse.

In this paper we use the atomic units.

2. Qualitative analysis of the amplitudes of high harmonic generation and above-threshold ionisation in strong low-frequency and weak high-frequency laser fields

Anticipating the analysis of the quasi-classical electron rescattering scenario in a strong low-frequency field with the assistance of a XUV photon, we make a number of qualitative remarks on the quantum-mechanical HHG and ATI amplitudes in a strong low-frequency laser field and in a weak (perturbative) field of a XUV pulse. We first consider the case when the XUV component of the laser field is determined by a monochromatic high-frequency field with a frequency Ω_γ and a strength F_γ. In our phenomenological analysis, we study the case of linear polarisation of both the low-frequency and high-frequency components of the field. Moreover, in our analysis we neglect various interference effects (see, for example, the analysis in [16]). The general expression for the HHG and ATI amplitudes in strong low-frequency and weak high-frequency fields can be written in the form:

$$A \approx A_{\mathrm{IR}} + A_{\mathrm{XUV}}(\Omega_\gamma),$$

where A_{IR} is the ATI/HHG amplitude in a strong low-frequency field, and $A_{\mathrm{XUV}}(\Omega_\gamma) \propto F_\gamma$ is the term determined by the XUV component of the field. Qualitatively, the amplitude A_{IR} can be represented as a product of three factors, i.e. tunnelling, propagation and atomic. The tunnelling factor is given by the tunnel exponential $\exp[-\kappa^3/(3F)]$, where κ specifies the ionisation potential of the atomic target, $I_\mathrm{p} = \kappa^2/2$; and F is the characteristic strength of the low-frequency laser field. The propagation factor depends smoothly on the harmonic frequency (in the case of HHG) or on the energy of photoelectrons (in the case of ATI) up to the cutoff energy (on the order of three ponderomotive potentials for HHG and ten ponderomotive potentials of the field for ATI). The atomic factor is determined by the photorecombination amplitude (for HHG) and the scattering amplitude (for ATI). Thus, in the absence of the XUV component, the height of the high-energy plateau in the HHG and ATI spectra is determined by the tunnelling probability, and the values of the cutoff energies are found from the quasi-classical rescattering scenario [1–4] (Fig. 1).

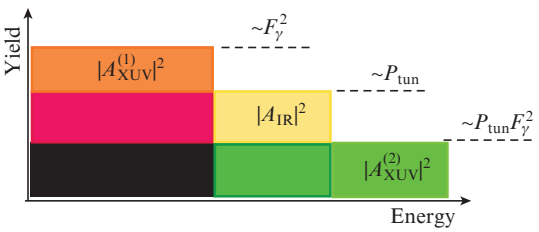

Figure 1. Schematic representation of the individual contribution to HHG and ATI of various rescattering channels in fields of intense low-frequency and weak XUV laser pulses ($P_{\mathrm{tun}} \propto \exp[-2\kappa^3/(3F)]$ is the probability of tunnelling ionisation).

The amplitude $A_{\mathrm{XUV}}(\Omega_\gamma)$ can be represented as the sum of two terms determining the partial amplitudes of the two channels induced by the interaction of the high-frequency field component with the atomic electron:

$$A_{\mathrm{XUV}}(\Omega_\gamma) = A_{\mathrm{XUV}}^{(1)}(\Omega_\gamma) + A_{\mathrm{XUV}}^{(2)}(\Omega_\gamma),$$

where $A_{\mathrm{XUV}}^{(1)}(\Omega_\gamma)$ and $A_{\mathrm{XUV}}^{(2)}(\Omega_\gamma)$ are the partial amplitudes corresponding to the first and second channels induced by XUV radiation (for details, see the Introduction). A qualitative analysis of the induced XUV channels also makes it possible to parametrize these partial amplitudes in the form of a product of three factors. Namely, the amplitude $A_{\mathrm{XUV}}^{(1)}(\Omega_\gamma)$ can be represented as the product of the photoionisation amplitude, the propagation factor with the modified cutoff energy (see Section 3) and the atomic factor determined by the recombination (in the case of HHG) and scattering (in the case of ATI) amplitudes. Thus, the main contribution from this channel is observed only if the probability of tunnelling is much less than the probability of single-photon absorption (Fig. 1). Note that in spite of the small (perturbative) intensity of the XUV component, such a situation can be realised experimentally. As will be shown in Section 3, a lower cutoff energy, than in the absence of a high-frequency component, corresponds to this channel.

Qualitatively, the partial amplitude $A_{\mathrm{XUV}}^{(2)}(\Omega_\gamma)$ can also be represented as the product of three factors: the tunnelling factor ($\propto\exp[-\kappa^3/(3F)]$), the propagation factor with a modified cutoff point with respect to energies of the harmonics and photoelectrons (see Section 4) and to XUV-modified recombination (in the case of HHG) and scattering (in the case of ATI) amplitudes. It is obvious that the contribution from this partial amplitude will be significantly suppressed; however, as shown in the analysis below (see Section 4), this channel leads to an increase in the cutoff energy, i.e., to the appearance of an additional plateau-like structure (Fig. 1).

Returning to the issue of the influence of the duration of a weak XUV pulse on the amplitude of high harmonic generation and above-threshold ionisation, we note that the amplitudes $A_{\mathrm{XUV}}^{(1)}(\Omega_\gamma)$ and $A_{\mathrm{XUV}}^{(2)}(\Omega_\gamma)$ linearly depend on the intensity F_γ. Thus, the result for a pulse of finite duration can be obtained by replacing F_γ by $F_\gamma(\Omega_\gamma)$ in the expressions for $A_{\mathrm{XUV}}^{(1)}(\Omega_\gamma)$ and $A_{\mathrm{XUV}}^{(2)}(\Omega_\gamma)$, followed by the integration of the obtained expressions in Ω_γ, where $F_\gamma(\Omega_\gamma)$ determines the spectral distribution of the XUV pulse intensity:

$$F_\gamma(t) = \int F_\gamma(\Omega_\gamma)\exp(-\mathrm{i}\Omega_\gamma t)\,\mathrm{d}\Omega_\gamma.$$

In the case of extremely short pulses, the width of the region of the largest contribution (in such integrals in Ω_γ) is of the same order of magnitude as the carrier frequency. However, if the pulse duration is five or more field periods, such a pulse can be considered with good accuracy monochromatic, and the qualitative results obtained for a monochromatic field will also be valid in the case of a pulse. It should be noted the high-frequency and low-frequency components can exhibit a phase difference, on which the shape of the HHG and ATI spectra substantially depend [17–20]. However, the present work is mainly aimed at analysing a more 'crude' effect, i.e. the appearance of new XUV-initiated plateau-like structures. This effect arises as a result of the dominance of one rescattering channel over the other and, accordingly, is determined by the square of the modulus of the partial amplitude of this

channel. Since the amplitudes $A^{(1)}_{\mathrm{XUV}}(\Omega_\gamma)$ and $A^{(2)}_{\mathrm{XUV}}(\Omega_\gamma)$ depend linearly on the field strength, their dependences on the relative phase φ can have the form $A^{(1,2)}_{\mathrm{XUV}}(\Omega_\gamma) \propto \exp(\mathrm{i}\varphi)$. Thus, the effects discussed below in the linear approximation in F_γ are independent of the relative phase between the low- and high-frequency components.

3. Quasi-classical scenario of rescattering with the absorption of a XUV photon by an electron in a bound state

In accordance with the first rescattering scenario, the first step is characterised by absorption of a XUV photon with a carrier frequency Ω_γ, which leads to the appearance of an electron with an energy $E_\mathrm{i} = \Omega_\gamma - I_\mathrm{p}$ in the continuum at the time $t = t_1$. The second step of the three-step rescattering scenario is the motion of an electron along a closed trajectory under the action of the field $\boldsymbol{F}(t)$ of the IR pulse. For the electron to return to the parent ion at the time $t = t_2$, it is necessary to satisfy the condition:

$$\frac{1}{2}[\boldsymbol{q}(t_1,t_2) + \boldsymbol{A}(t_1)]^2 = \Omega_\gamma - I_\mathrm{p} = E_\mathrm{i}, \tag{1}$$

$$\boldsymbol{q}(t_1,t_2) = -\frac{1}{t_2 - t_1}\int_{t_1}^{t_2} \boldsymbol{A}(t)\,\mathrm{d}t, \tag{2}$$

where $\boldsymbol{A}(t)$ is the vector potential of the low-frequency laser field [$\boldsymbol{F}(t) = -\dot{\boldsymbol{A}}(t)$]. Equation (1) reflects the equality of the kinetic energy of the electron in the field $\boldsymbol{F}(t)$ at time t_1 with energy E_i obtained by the electron after absorption of a photon with energy Ω_γ. Expression (2) for the 'momentum' $\boldsymbol{q}(t_1, t_2)$ provides a closed trajectory of the electron motion and corresponds to the solution of the classical equation of motion $\ddot{\boldsymbol{r}} = -\boldsymbol{F}(t)$ with uniform boundary conditions $\boldsymbol{r}(t_1) = \boldsymbol{r}(t_2) = 0$:

$$\boldsymbol{r}(t) = \boldsymbol{q}(t_1,t_2)(t - t_1) + \int_{t_1}^{t} \boldsymbol{A}(t)\,\mathrm{d}t.$$

We note that at $\Omega_\gamma = 0$, equation (1) coincides with the corresponding equation for the rescattering scenario obtained in the analysis of the quantum HHG and ATI amplitudes in the quasi-classical approximation for the case of the IR pulse. If $E_\mathrm{i} \sim I_\mathrm{p}$, then equation (1) can be solved by perturbation theory methods with respect to the parameter $\gamma = \omega\sqrt{2(\Omega_\gamma - I_\mathrm{p})}/F$, where ω and F are the carrier frequency and peak field intensity of the low-frequency pulse (this procedure is analogous to that considered in [14] for the case of an IR pulse, where the Keldysh parameter plays the role of the smallness parameter, $\gamma_\mathrm{K} = \omega\sqrt{2I_\mathrm{p}}/F$).

An additional equation for the pair of times t_1, t_2 depends on the final state of the quantum system and, accordingly, on the process in question. For HHG, the third step of the rescattering pattern is the recombination of the electron into the ground state of the atom with the emission of a harmonic photon with the energy Ω_HHG. The equality of the kinetic energy of the electron in the field $\boldsymbol{F}(t)$ at the time t_2 and the recombination energy determines this additional equation:

$$\frac{1}{2}[\boldsymbol{q}(t_1,t_2) + \boldsymbol{A}(t_2)]^2 = \Omega_\mathrm{HHG} - I_\mathrm{p}. \tag{3}$$

In the case of ATI, equation (3) should be replaced by the law of conservation of the free-electron energy in the laser field $\boldsymbol{F}(t)$ at the time of rescattering t_2 with changing the momentum $\boldsymbol{q}(t_1, t_2)$ to the asymptotic momentum $\boldsymbol{p}$ of the final state:

$$\frac{1}{2}[\boldsymbol{q}(t_1,t_2) + \boldsymbol{A}(t_2)]^2 = \frac{1}{2}[\boldsymbol{p} + \boldsymbol{A}(t_2)]^2. \tag{4}$$

The system of coupled equations (1) and (3) for HHG or (1) and (4) for ATI determines the moments of the initial (t_1) and final (t_2) times when a free electron moves along a closed trajectory in the field of a low-frequency laser pulse between the moments of ionisation and recombination (for HHG) or rescattering (for ATI). This system of equations determines the quasi-classical rescattering model in accordance with the first scenario corresponding to the absorption of a hard photon at the first step. We note that, as part of the considered quasi-classical rescattering model, the influence of the atomic potential on the motion of an electron between collisions with an atom is neglected. The influence of the high-frequency pulse field is taken into account by the presence of the term Ω_γ in the right-hand side of equation (1), which is absent in the case of a single IR pulse.

Let us find the real solutions t_1, t_2, corresponding to the maximum values of the energy of the radiated harmonic Ω_HHG and rescattered electron $E = p^2/2$. These values determine the plateau cutoff position in the HHG and ATI spectra. The systems of equations for t_1 and t_2, corresponding to $\max\Omega_\mathrm{HHG}$ and $\max E$, are obtained by combining equation (1) with one of the following equations:

$$\frac{\mathrm{d}}{\mathrm{d}t_2}\Omega_\mathrm{HHG}[t_1(t_2), t_2] = 0, \tag{5}$$

$$\frac{\mathrm{d}}{\mathrm{d}t_2}E[t_1(t_2), t_2] = 0, \tag{6}$$

where Ω_HHG and E are considered as functions of time given by equations (3) and (4), respectively, and the total derivative with respect to the variable t_2 is calculated taking into account the implicit dependence $t_1 = t_1(t_2)$ according to equation (1).

In what follows we confine ourselves to the case of linear polarisation of the field $\boldsymbol{F}(t)$:

$$\boldsymbol{F}(t) = \boldsymbol{e}Ff(\omega t), \quad \boldsymbol{A}(t) = \boldsymbol{e}\frac{F}{\omega}a(\omega t),$$

where $f(\tau)$ and $a(\tau)$ are dimensionless functions that determine the evolution of the low-frequency field intensity and vector potential, respectively; $f(\tau) = -\mathrm{d}a/\mathrm{d}\tau$; $\tau \equiv \omega t$; and $\boldsymbol{e}$ is the unit polarisation vector.

Let us first consider the case of HHG and obtain an expression for the maximum energy of the photon of the harmonic $\max\Omega_\mathrm{HHG}$. In the zeroth approximation with respect to the small parameter γ, equations (1) and (5) take the form [15]:

$$a(\tau_1) - \frac{1}{\tau_2 - \tau_1}\int_{\tau_1}^{\tau_2} a(\tau)\,\mathrm{d}\tau = 0, \tag{7}$$

$$f(\tau_2) + \frac{a(\tau_2) - a(\tau_1)}{\tau_2 - \tau_1} = 0. \tag{8}$$

The joint solution of equations (7) and (8) gives the times of the beginning and the end of the motion along closed extremal trajectories on which Ω_{HHG} takes maximum values. A global maximum for the case of the monochromatic field $f(\tau) = \cos\tau$ is reached at times $\tau_2 - \tau_1 = 4.086$ and $\tau_2 + \tau_1 = \pi/2$, which correspond to the shortest (single-return) trajectory.

Using the procedure of the iterative solution of equations (1) and (5), described in [15], we obtain to within terms $\sim\gamma^2$ the expression

$$\max \Omega_{\mathrm{HHG}} = 2u_{\mathrm{p}}[a(\tau_2) - a(\tau_1)]^2 + \frac{f(\tau_2)}{f(\tau_1)}(\Omega_\gamma - I_{\mathrm{p}}), \qquad (9)$$

where τ_1 and τ_2 are determined by the system of equations (7) and (8); and u_{p} is the ponderomotive energy of an electron in a strong laser field. For a monochromatic field, expression (9) takes the form

$$\max\Omega_{\mathrm{HHG}} = 3.17u_{\mathrm{p}} - 0.324(\Omega_\gamma - I_{\mathrm{p}}). \qquad (10)$$

Relationships (9) and (10) indicate a linear dependence of the high-energy plateau cutoff position in the HHG spectrum on the carrier frequency of the high-frequency pulse Ω_γ. To this end, the analysis of the solutions of Eqns (7) and (8) shows that $f(\tau_2)/ f(\tau_1) < 0$ in the plateau cutoff region, and, consequently, an increase in the carrier frequency of the high-frequency pulse leads to a shortening of the high-energy plateau.

Figure 2 shows the dependences of the maximum energy of the emitted photon of the harmonic on the carrier frequency of the high-frequency pulse for the case of a monochromatic IR field. The solid curve is the result of the exact solution of the system of equations (1) and (5) for the times t_1, t_2, which are a point of the global maximum of the function $\Omega_{\mathrm{HHG}}(t_1, t_2)$ in (3); the dashed curve is the approximate result of (10). As can be seen from the figure, the analytical solution (10) agrees perfectly with the result of an accurate calculation up to $\Omega_\gamma = I_{\mathrm{p}} + 1.5u_{\mathrm{p}}$ and shows a linear decrease in the high-energy plateau cutoff position with increasing carrier frequency of the high-frequency pulse. A further growth of Ω_γ leads to a sharp reduction in the plateau when HHG is realised through ionisation of the atomic target during XUV photon absorption. At $\Omega_\gamma > 3.17u_{\mathrm{p}} + I_{\mathrm{p}}$, real solutions to equations (1) and (5) do not exist.

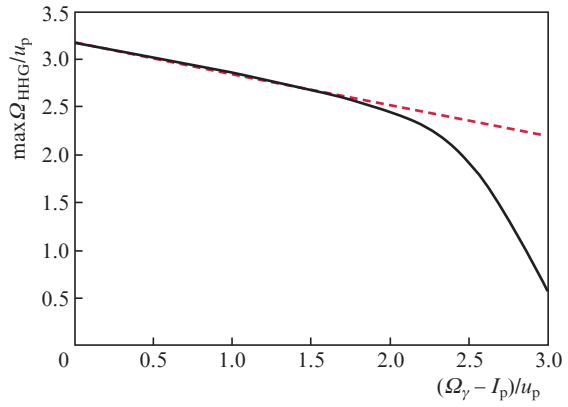

Figure 2. Dependence of the maximum photon energy of the harmonic $\max\Omega_{\mathrm{HHG}}$ on the carrier frequency Ω_γ of the XUV pulse according to the first rescattering scenario. The solid curve is the exact result of solving equations (1), (3) and (5), and the dashed curve is the approximate result for (10).

The analysis of ATI and derivation of a relation for the maximum photoelectron energy are carried out in a manner analogous to that described above for HHG. Let us consider the case of the collinear geometry $\boldsymbol{e}\|\boldsymbol{p}$. The equations for the times of the beginning and the end of the motion along the extremal trajectories corresponding to the maximal energies $\max E$ in the zeroth approximation with respect to the parameter γ formally coincide with the system of equations (7), (8) with the replacement $f(\tau_2) \to 2f(\tau_2)$ in equation (8) (cf. with [14] for the case of a single IR pulse):

$$2f(\tau_2) + \frac{a(\tau_2) - a(\tau_1)}{\tau_2 - \tau_1} = 0. \qquad (11)$$

An iterative solution of the system of equations (1) and (6) with respect to the parameter γ leads to the following result:

$$\max E = 2u_{\mathrm{p}}(|a(\tau_2)| + |a(\tau_2) - a(\tau_1)|)^2 + 4\frac{f(\tau_2)}{f(\tau_1)}\left(1 + \frac{|a(\tau_2)|}{|a(\tau_2) - a(\tau_1)|}\right)(\Omega_\gamma - I_{\mathrm{p}}), \qquad (12)$$

where the times τ_1 and τ_2 are determined by the system of equations (7) and (11). For the monochromatic field, relation (12) takes the form:

$$\max E = 10u_{\mathrm{p}} - 0.54(\Omega_\gamma - I_{\mathrm{p}}). \qquad (13)$$

One can see from (12) and (13) that similarly to the HHG case, the maximum photoelectron energy decreases linearly with increasing photon energy of the high-frequency pulse.

Figure 3 shows the dependence of the maximum energy of the rescattered electrons on the carrier frequency of the high-frequency pulse for the case of a monochromatic IR field. The solid curve is the result of the exact solution of the system of equations (1) and (6) for the point (t_1, t_2) of the global maximum of the function $E(t_1, t_2)$ implicitly given by equation (4); the dashed curve is the approximate result of (13). As in the case of harmonic generation (see Fig. 2), there is a linear decrease in the energy of rescattered electrons with increasing Ω_γ in the region $\Omega_\gamma = I_{\mathrm{p}} + 1.5u_{\mathrm{p}}$. With a further increase in Ω_γ, the energy of rescattered electrons decreases rapidly, so that the considered rescattering mechanism becomes ineffective.

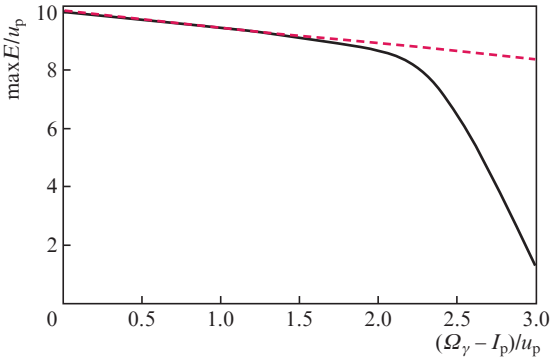

Figure 3. Dependence of the maximal energy $\max E$ of photoelectrons on the carrier frequency Ω_γ of the XUV pulse according to the first rescattering scenario. The solid curve is the exact result of solving equations (1), (4) and (6), and the dashed curve is the approximate result for (13).

Thus, the first rescattering scenario, in which the high-frequency pulse ionises the atomic target at the first step, leads to a linear shortening of the high-energy plateau with increasing XUV carrier frequency for both the HHG and ATI processes.

4. Quasi-classical scenario of rescattering with absorption of a XUV photon at the moment of recombination

Let us consider the second scenario of the modification of HHG and ATI spectra, namely, the case when the XUV photon is emitted/absorbed at the third step of the three-step rescattering mechanism, i.e., when the active electron recombines with the parent ion in the HHG process or electron–ion rescattering occurs in the ATI process.

According to the quasi-classical rescattering scenario for the HHG process, an electron at the first step tunnels from the atom and leaves at the time t_1 for the zero-energy continuum, moving along the closed trajectory. This step can be characterised by the equation

$$\boldsymbol{q}(t_1, t_2) + \boldsymbol{A}(t_1) = 0 \tag{14}$$

coinciding with equation (1) for the first rescattering scenario at $E_i = 0$ [the case of linear polarisation of the field $\boldsymbol{F}(t)$ is considered]. At time t_2, the IR laser field $\boldsymbol{F}(t)$ returns the electron to the ion, where the electron recombines to the bound state. Recombination occurs in the presence of a XUV-pulse field and can be accompanied by additional emission or absorption of a photon with energy Ω_γ. The following classical equation of conservation of energy corresponds to this recombination step:

$$\frac{1}{2}[\boldsymbol{q}(t_1, t_2) + \boldsymbol{A}(t_2)]^2 = \Omega_{\mathrm{HHG}} \pm \Omega_\gamma - I_p. \tag{15}$$

In equation (15), the sign '+' ('–') corresponds to recombination with additional emission (absorption) of the XUV photon. The equation for the photon energy extremum of the harmonic Ω_{HHG} as a function of the recombination time does not depend on the value of Ω_γ and coincides with equation (8). Thus, a weak high-frequency pulse has no effect on closed classical trajectories that determine the HHG amplitude in the case of a single IR pulse in the quasi-classical approximation. It follows from Eqn (15) that the second rescattering scenario for HHG leads to linear extension [sign '–' in Eqn (15)] or to shortening (sign '+' in the same equation) of the high-energy plateau as the carrier frequency of the high-frequency pulse increases.

For ATI (as for HHG), the first step in the rescattering process is the electron tunnelling at time t_1 to the continuum described by Eqn (14). At time t_2 of the rescattering of the electron from the parent ion, the kinetic energy of the electron in the IR field, corresponding to the field-induced momentum $\boldsymbol{q}(t_1, t_2)$, undergoes a transition into the kinetic energy, corresponding to the asymptotic (finite) momentum $\boldsymbol{p}$, increased or decreased by the XUV photon energy Ω_γ:

$$\frac{1}{2}[\boldsymbol{q}(t_1, t_2) + \boldsymbol{A}(t_2)]^2 = \frac{1}{2}[\boldsymbol{p} + \boldsymbol{A}(t_2)]^2 \pm \Omega_\gamma. \tag{16}$$

It follows from Eqn (16) that absorption or emission of a high-frequency photon, respectively, decreases or increases the energy of rescattered electrons. It should be emphasised that in (16) the smallness of the XUV-photon energy with respect to the average quiver energy u_p of an electron in a strong IR field is not assumed. Similarly to the rescattering scenario discussed in Section 2, in order to find the maximum, classically permissible, photoelectron energy max$E$, it is necessary to differentiate equation (16) with respect to t_2, taking into account the implicit dependence $t_1 = t_1(t_2)$ given by equation (14), and assuming $\mathrm{d}E/\mathrm{d}t_2 = \boldsymbol{p}\mathrm{d}\boldsymbol{p}/\mathrm{d}t_2 = 0$. As a result, we obtain the equation (we consider the case of the collinear geometry $\boldsymbol{e} \| \boldsymbol{p}$):

$$\boldsymbol{F}(t_2)\left[1 + \left(1 \pm \frac{2\Omega_\gamma}{[\boldsymbol{A}(t_2) - \boldsymbol{A}(t_1)]^2}\right)^{1/2}\right] + \frac{\boldsymbol{A}(t_2) - \boldsymbol{A}(t_1)}{t_2 - t_1} = 0. \tag{17}$$

The system of equations (14) and (17) determines the times of the beginning and the end of the electron motion in the field $\boldsymbol{F}(t)$ along closed extremal trajectories. These times are modified by a high-frequency pulse for XUV-photon energies exceeding the ponderomotive energy of an electron in a low-frequency field: $\Omega_\gamma > u_p$. This fact is illustrated in Fig. 4, where it is shown how the XUV pulse affects the return time $\Delta t = t_2 - t_1$ of the electron to the parent ion. For 'soft' photons (such that $\Omega_\gamma \lesssim u_p$), the influence of the high-frequency pulse on the times t_1, t_2 can be neglected.

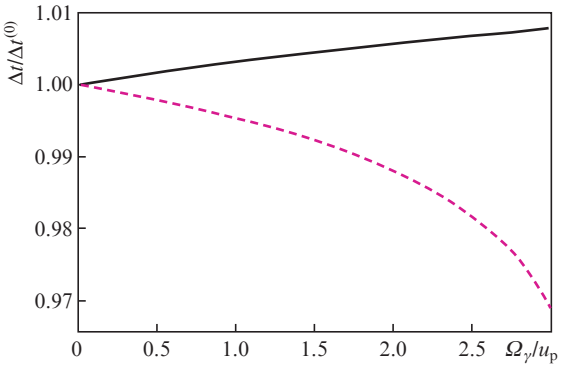

Figure 4. Time $\Delta t = t_2 - t_1$ of the electron motion along the shortest extremal trajectory between the moments of tunnelling t_1 and rescattering t_2 as a function of the carrier frequency Ω_γ of the XUV pulse with respect to the corresponding time $\Delta t^{(0)} = 4.306\omega^{-1}$ of motion in the absence of the XUV pulse. The solid curve corresponds to absorption of the XUV photon, and the dashed curve corresponds to its emission.

The result for the maximum energy max$E$ of the rescattered electrons follows from equation (16) with allowance for equation (14):

$$\max E = \frac{1}{2}\left(|\boldsymbol{A}(t_2)| + \sqrt{[\boldsymbol{A}(t_2) - \boldsymbol{A}(t_1)]^2 \mp 2\Omega_\gamma}\right)^2, \tag{18}$$

where the times t_1, t_2 are the solution to the system of equations (14) and (17), and the sign '–' ('+') corresponds to absorption (emission) of the VUV photon in the process of rescattering. It follows from (18) that in contrast to the first rescattering scenario, the linear dependence of the high-energy plateau cutoff in the ATI spectra on the carrier frequency of the high-frequency pulse should be observed only in the case of 'soft' photons when the condition $\Omega_\gamma \ll u_p$ is satisfied.

Figure 5 shows the dependence of the maximum energy of the rescattered electrons on the carrier frequency of the high-frequency pulse in accordance with Eqn (18) for the second rescattering scenario with emission or absorption of the XUV photon at the rescattering step. As can be seen from the figure, the linear dependence of the high-energy plateau cutoff on Ω_γ in the ATI spectra should be observed up to $\Omega_\gamma \sim u_p$.

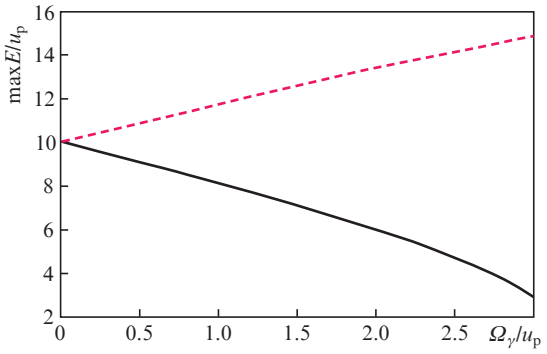

Figure 5. Dependence of the maximum energy max$E$ of photoelectrons on the carrier frequency Ω_γ of the XUV pulse according to the second rescattering scenario. The solid curve corresponds to absorption of the VUV photon, and the dashed curve corresponds to its emission.

5. Conclusions

The analytical relationships presented in this paper make it possible to estimate the plateau cutoff positions in the HHG and ATI spectra in u_p units of an average vibrational energy of a free electron in an intense IR field. As an example of application of the estimates obtained, we can consider the interaction of an electron in the ground state of a hydrogen atom ($I_p = 13.6$ eV) with a monochromatic (picosecond) laser pulse with an intensity $I = 10^{14}$ W cm^{-2} and a wavelength $\lambda = 2$ μm ($u_p = 37.35$ eV). For these conditions, the Keldysh parameter is $\gamma_K = 0.6$.

The quasi-classical electron rescattering model in an intense low-frequency field allows one to obtain simple estimates for the boundaries of a high-energy plateau in the spectra of field-induced HHG and ATI processes. The inclusion of an additional weak XUV pulse substantially modifies the spectra of the processes by one of two possible mechanisms: 1) the XUV photon is absorbed at the first rescattering step, transferring the active electron to the continuum and replacing the tunnelling process in the case of a standard three-step rescattering model; and 2) the XUV-photon–high-frequency pulse exchange occurs at the step of rescattering or recombination of an electron. In the case of the first rescattering scenario, a close-to-linear decrease in the maximum, classically allowed, photon energy of the harmonic and the photoelectron is observed for the considered HHG and ATI processes, while for the second scenario both a decrease in this energy and an increase in it are possible, depending on whether the XUV photon is absorbed or emitted in the process of recurrent collision of an electron with an atom. Thus, a change in the carrier frequency of a high-frequency pulse makes it possible to modify the boundary of a high-energy plateau and also to separate various mechanisms responsible for generating harmonics or obtaining high-energy electrons.

Acknowledgements. The work was supported by the Russian Science Foundation (Grant No. 15-12-10033).

References

1. Kuchiev M.Yu. *Pis'ma Zh. Eksp. Teor. Fiz.*, **45**, 319 (1987) [*JETP Lett.*, **45**, 404 1987)].
2. Shafer K.J., Yang B., DiMauro L.F., Kulander K.C. *Phys. Rev. Lett.*, **70**, 1599 (1993).
3. Corkum P.B. *Phys. Rev. Lett.*, **71**, 1994 (1993).
4. Paulus G.G., Becker W., Nicklich W., Walther H. *J. Phys. B*, **27**, L703 (1994).
5. Fleischer A., Moiseyev N. *Phys. Rev. A*, **77**, 010102(R) (2008).
6. Fleischer A. *Phys. Rev. A*, **78**, 053413 (2008).
7. Popruzhenko S.V., Zaretsky D.F., Becker W. *Phys. Rev. A*, **81**, 063417 (2010).
8. Leeuwenburgh J., Cooper B., Averbukh V., Marangos J.P., Ivanov M. *Phys. Rev. Lett.*, **111**, 123002 (2013).
9. Brown A.C., van der Hart H.W. *Phys. Rev. Lett.*, **117**, 093201 (2016).
10. Corkum P.B., Krausz F. *Nat. Phys.*, **3**, 381 (2007).
11. Krausz F., Stockman M. *Nat. Photonics*, **8**, 205 (2014).
12. Hentschel M., Kienberger R., Spielmann Ch., Reider G.A., et al. *Nature*, **414**, 509 (2001).
13. Uiberacker M., Uphues Th., Schultze M., Verhoef A.J., et al. *Nature*, **446**, 627 (2007).
14. Frolov M.V., Manakov N.L., Popov A.M., Tikhonova O.V., et al. *Phys. Rev. A*, **85**, 033416 (2012).
15. Frolov M.V., Knyazeva D.V., Manakov N.L., Geng J.-W., et al. *Phys. Rev. A*, **89**, 063419 (2014).
16. Frolov M.V., Manakov N.L., Xiong W.H., Peng L.Y., et al. *Phys. Rev. A*, **92**, 023409 (2015).
17. Bandrauk A.D., Shon N.H. *Phys. Rev. A*, **66**, 031401(R) (2002).
18. Shafer K.J., Gaarde M.B., Heinrich A., Biegert J., et al. *Phys. Rev. Lett.*, **92**, 023003 (2004).
19. Biegert J., Heinrich A., Hauri C.P., et al. *Laser Phys.*, **15**, 899 (2005).
20. Johnsson P., López-Martens R., Kazamias S., Mauritsson J., et al. *Phys. Rev. Lett.*, **95**, 013001 (2005).